Proceedings of the 26th International Conference on
Port and Ocean Engineering under Arctic Conditions
June 14-18, 2021, Moscow, Russia

Field experiments on collisional interaction of floating ice blocks

Marchenko, A.V.[1], Chistyakov, P.V.[2], Karulin, E.B.[3], Markov, V.V.[2,4], Morozov, E.G.[5], Karulina, M.M.[3], Sakharov, A.N.[2]
[1]The University Centre in Svalbard, Longyearbyen, Norway
[2]Lomonosov Moscow State University, Moscow, Russia
[3]Krylov State Research Center, St. Petersburg, Russia
[4]Steklov Mathematical Institute of RAS, Moscow, Russia
[5]Shirshov Institute of Oceanology of RAS, Moscow, Russia

ABSTRACT

Field experiments were performed to investigate collisional interaction of ice floes and characteristics of water currents between interacting floes. The experiments were organized in the Van-Mijen Fjord in Spitsbergen in the winter season of 2019. In the first experiment an ice block was hanged on an iron rig by a chain as a pendulum. In the rest position the ice block was submerged in the water in artificially made pool and had a contact with ice edge of land fast ice. The accelerations of the ice block were recorded after it was replaced from the rest position and released. In the second experiment a floe with sizes 5 m x 10 m was made in a pool with sizes 5.5 m x 12 m. The floe motion along the pool back and forward was initiated by mechanical pooling by a rope. During the experiments we recorded the floe acceleration and water velocity below the ice. The experimental data were used to describe properties of floe-floe collisions and characteristics of water motion initiated by floe motion and floe-floe interactions.

KEY WORDS: floe, collision, acceleration, turbulence

INTRODUCTION

Numerous papers are devoted in the investigation of collisional interaction of immersed particles with each other and with solid walls. Theoretical consideration of a sphere near a solid wall in ideal incompressible fluid leads to the conclusion that direct contact between the sphere and wall is not possible due to the action of the water pressure (Lamb, 1975). Starovoitov (2003) investigated theoretically this problem in the case when the motion occurs in incompressible viscous fluid and concluded that the body approaches the wall with zero velocity or cannot touch it at all. Tchieu et al (2010) investigated numerically the interaction of two cylinders submerged in ideal incompressible fluid. They found that central collision is not realized, and cylinders can change trajectories to avoid direct contact in case if they approach each other not along the line connecting their centers.

Devis et al (1986) investigated the influence of elastic properties on the collisional interaction of bodies. He concluded that rebound of the approaching bodies can be realized without their direct contact. The rebound velocity and restitution coefficient are controlled by the Stokes ($\sim\rho_p Re/\rho$) and Reynolds ($\sim\rho v_0 d/\mu$) numbers, where ρ_p and ρ are the densities of particles and water, v_0 is the relative velocity, d is the diameter of particles, and μ is the fluid viscosity. Joseph et al (2001) investigated particle-wall collisions in viscous fluid experimentally for the particles made of different materials. It was revealed that rebound velocity decreases with the decreasing the Stokes number. It controls the diameter of particles allowing the direct contact by the interaction. Large effective viscosity of grease ice (De Carolis et al., 2005) influences large sizes of particles interacting without collisions in cold waters.

Wave induced ice floes collisions were investigated using the data of in-situ (Martin and Becker, 1987) and laboratory (Li and Lubbad, 2018) experiments. Martin and Becker (1987) concluded that the mean square velocity associated with collisions was 1 mm/s, and ice floe collisions are not strong enough to contribute strongly to the ice deformation. Li and Lubbad (2018) concluded that wave energy dissipated by collisions is significant. Marchenko et al. (2019) investigated dry and wet collisions of ice blocks with floating ice in the field experiments. They found that representative time of dry collision of ice cube with flat floating ice is of the order of 0.01 s with the maximal relative acceleration greater than 40 g. The representative time of wet collision of the ice pyramid with floating ice is estimated to be about 0.15 s with the maximal acceleration of the pyramid of 5 g. Numerical modeling confirmed that in the wet collision the energy of ice pyramid was transferred into the kinetic energy of water volume forming a spray due to the collision.

In the present paper we describe preliminary results of the field tests where ice-ice collisions were realized both by the pendulum method and by the direct puling of floe by a rope. In both experiments the collisions occurred in the water. The sizes of colliding ice masses were large enough to demonstrate importance of the ice shape and sizes on the collision process. The influence of water was also important for energy dissipation and damping.

INELASTIC COLLISION OF A FLOE WITH A SOLID WALL

Floes interact with obstacles (other floes and constructions) by collisions. Energy dissipation during collisions is associated both with fracture and viscous deformations of ice and with water-ice interaction. Energy losses during the collisions make them inelastic. Figure 1 shows qualitative description of the dependencies of velocities and accelerations of the point O of circular floe from time during the collision. Any other point of the floe has similar motion because of the symmetry. The collision happens if the floe velocity changes sign. It is assumed that the floe velocity equals v_0 before the collision, and velocity approaches to $v_1 \leq 0$ after the collision. Thin line in Fig. 1b corresponds to ideal elastic collision when $v_1 = -v_0$, and viscous-elastic collision when $v_1 = v_{1,0} > -v_0$. Thick line in Fig. 1b corresponds to the collision in the water. The water action influences a reduction of the floe speed immediately after the collision.

Figure 1c shows accelerations versus time. The integral from acceleration with respect to time equals to the change of the velocity. Thin line around dark gray region corresponds to the acceleration at the thin line in Fig. 1b. The area of dark gray region equals $v_0 - v_{1,0}$. Thick line in Fig. 1c corresponds to the acceleration at the thick line in Fig. 1b. The area of light gray region equal to $v_0 - v_1$ is smaller than the area of the dark gray region because light gray areas above and below axis t are accounted with different signs.

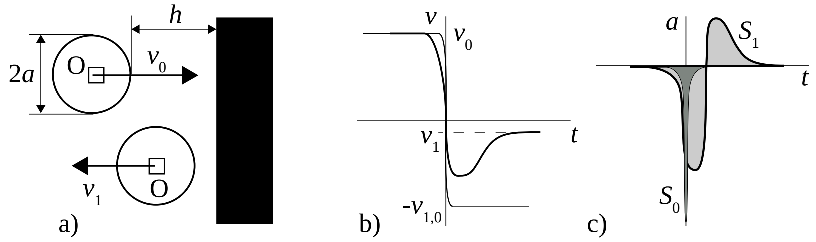

Figure 1. Inelastic collision of disk with a wall (a). Qualitative dependencies of the disk velocity (b) and acceleration (c) on time during the collision.

Figure 2 illustrates the time dependence of the velocity and acceleration of arbitrary point O of rectangular floe when it collides with a wall. This interpretation is important for the understanding of accelerometer records in the field experiments. It is assumed that the accelerometer is installed at point O which doesn't coincide with the point of the first contact of the floe with the wall. After the first contact the floe stops and begins to rotate relative to the contact point.

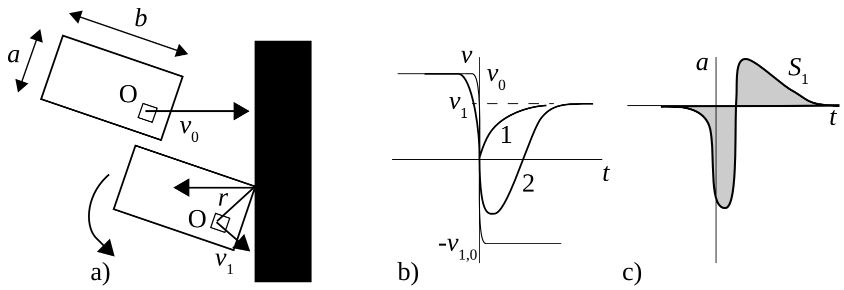

Figure 2. Inelastic collision of a rectangular body with a wall (a). Qualitative dependencies of the rectangle velocity (b) and acceleration (c) on time during the collision.

The speed of point O can be estimated using the assumption that the kinetic energy of translational floe motion is equal to the kinetic energy of the rotational motion. It leads to the formula $v_0^2 = \omega^2(a^2 + b^2)/12$, where v is the floe velocity before the collision, ω is the angular floe velocity after the collision, and a and b are the floe sizes (Fig. 2). The speed v_1 of point O after the collision equals ωr, where r is the distance between the contact point and point O. Thus, we have

$$v_1 = 2v_0\sqrt{3r^2/(a^2 + b^2)}. \tag{1}$$

In case if $r = a = b$ we find $v_1 = 2.5v_0$, i.e., rotational velocity of the floe points can be higher than the velocity of their translational motion before the collision. Qualitative dependence of velocity v_1 on time after the collision is shown by line 1 in Fig. 2b. Line 2 shows the dependence of velocity v_1 on time in the case when rebound occurs, the floe velocity changes the sign, and the influence of water drag influences floe rotation. Figure 2c shows qualitative dependence of the acceleration of point O in the case when the floe rotates after the collision. It looks similar Fig. 1c, but the area of the gray region above the axis t is larger than in Fig. 1c. Total area of the gray region in Fig. 2c is equal to zero when $v_1 = v_0$.

PENDULUM EXPERIMENT WITH ICE BLOCK

An ice block of rectangular shape with a size of about 0.5 m was cut from sea ice and mounted on a L shape frame by ice screws and a chain (Fig. 3). During the experiment the block was submerged in a pool with a size of 2m x 5m and collided with the vertical edge of floating sea ice. The collision was initiated by initial displacement of the block to the side from the ice edge by a rope and consequent release of the rope. The motion of the submerged block continued until the block collided with the ice edge. The block motion was recorded by video and the block acceleration was measured by the uniaxial accelerometer Bruel & Kjær DeltaTron Type 8344 with a sampling interval of 0.2 ms.

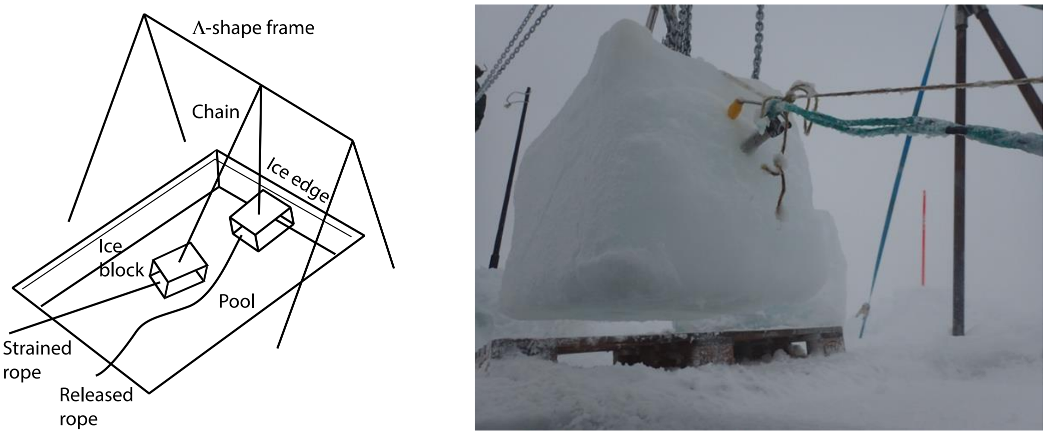

Figure 3. Schematic of pendulum experiment with ice block (left panel). Ice block with rope used in the experiment (right panel).

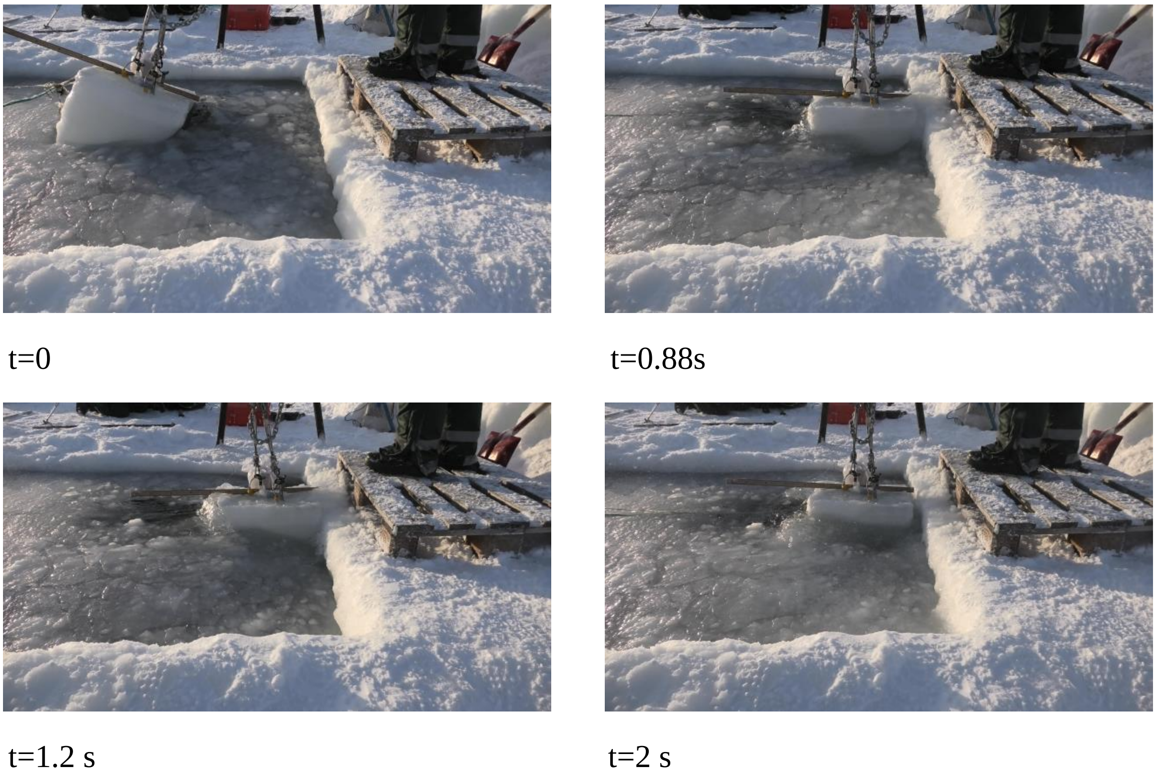

Figure 4. Fragments of the block position reconstructed from video file.

Four video frames in Fig. 4 show the beginning of the test (t=0) and the collision process. The water surface was covered by slush in the pool. The motion of block influences cleaning of the water surface from slush behind the block, splashing of water on the ice edge, and formation of surface waves. The collisional interaction extended over about 0.2 s. Wave reflection from the ice edge influenced the motion of ice block in the opposite direction after the collision. Separation of the block from the ice edge is seen in Fig. 1 at time moment t=2s.

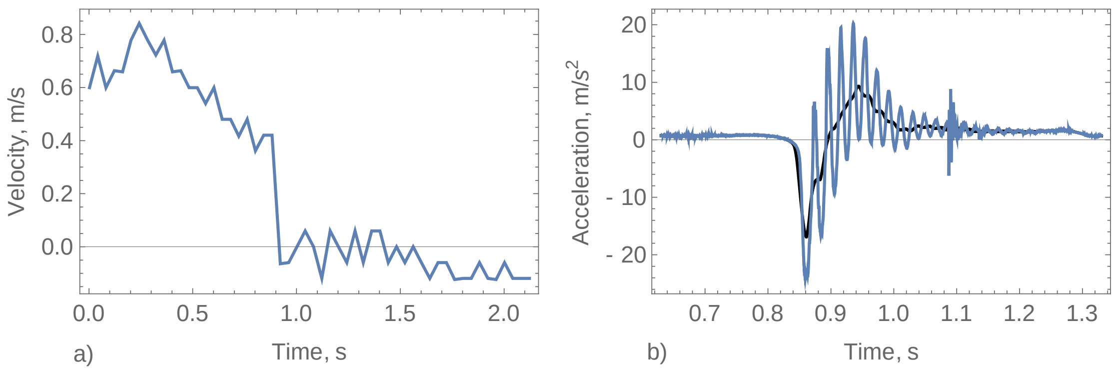

Figure 5. Horizontal velocity of the ice block versus time reconstructed from the video (a). Measured (blue line) and averaged (black line) accelerations versus time (b).

The horizontal velocity of the ice block reconstructed by consequent analysis of the video frames is shown by the blue line in Fig. 5a. One can see that after the rope allows the free block motion, the block velocity increases during 0.3 s and then decreases. Just before the collision the block velocity is estimated lower than 0.8 m/s. The velocity dropped to zero over 0.1 s, and after that the block was "glued" to the wall over 0.5 s. Rebounds were not observed. The inverse motion of the block was initiated by reflected wave by t>1.5s. The blue line in Fig. 5b shows the recorded acceleration versus the time. The black line shows running averaged values of the recorded acceleration. We think that positive accelerations recorded by t>0.9 s are related to the rotational motion of the block relatively the contact points of the block with ice edge. The oscillations with a period of about 50 Hz in Fig. 5b can be explained by vibrations of the wooden block with the accelerometer mounted to the ice block by screws.

FLOE DRIFT EXPERIMENT

A floe of rectangular shape was cut by Ditch Witch trencher in land fast ice of Vallunden Lake in the Van Mijen Fjord (Spitsbergen) on March 11, 2019 (Fig. 6). The ice thickness was 80 cm, and the floe size was 5m x 10m. The size of a pool where the floe was floating was 12m x 5.5m. Lake Vallunden is connected to the Van Mijen Fjord by a strait of 100 m length and 10-20 m width. Tidal jet penetrating through the strait provides strong mixing of fjord water and lake water (Morozov et al., 2019). Since there are no regular fresh water supply to the lake by rivers, the lake is filled with sea water with a salinity of 34 ppt. Sea ice in the lake has columnar structure and belong to S2 type. The range of the influence of the tidal jet is approximately 200 m from the strait. The pool with the floe was located at the distance greater than 300 m from the lake. Although the water surface elevation due to the semidiurnal tide reaches 10-20 cm in the lake the currents were not recorded in the lake during the ice season at distances greater than 200 m from the strait.

A sketch of the drift floe experiment is shown in Fig. 7. The experiment was focused on the investigation of water motion caused by the floe motion in the pool. The floe motion was initiated by consequent manual pooling of two ropes fixed at the floe edges. The floe motion was recorded by two accelerometers (Bruel & Kjær DeltaTron Type 8344) mounted to the floe at two locations marked by A1 and A2 in Fig. 7. The sampling frequency of accelerometers was set to 100 Hz. Three components of the water velocity were measured by ocean probe

ADV SonTek Hydra 5 MHz with sampling frequency 10 Hz at the three locations marked by ADV1,2,3 in Fig. 7.

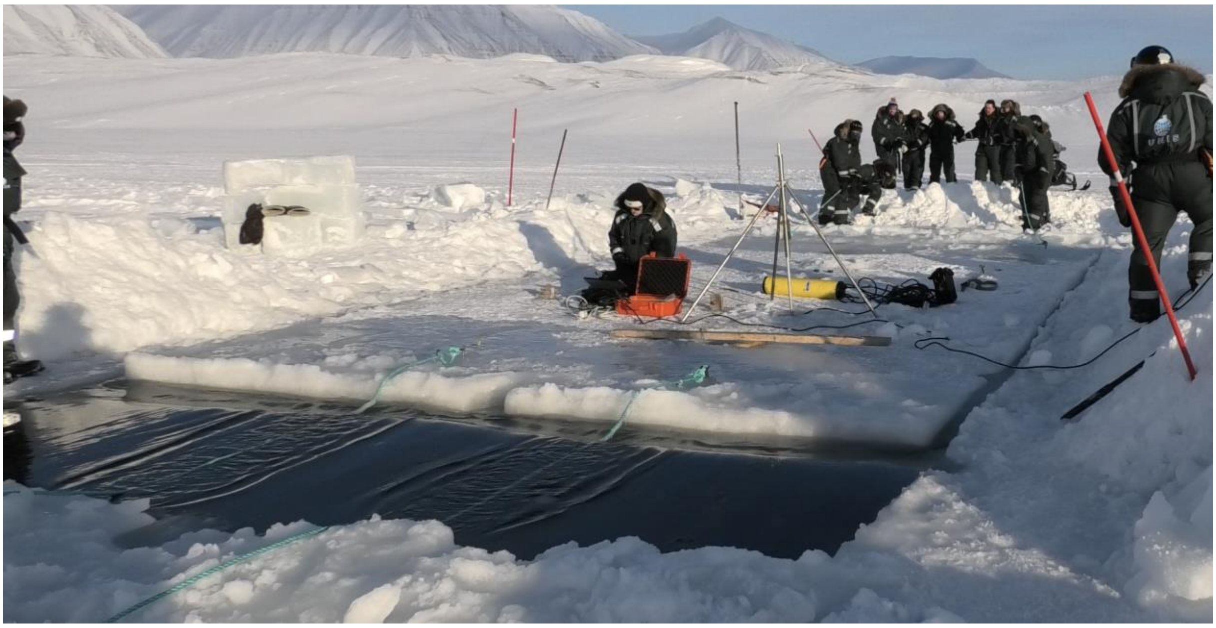

Figure 6. Photograph of drift floe experiment. Vallunden Lake, Van-Mijen Fjord, Spitsbergen, March 12, 2019.

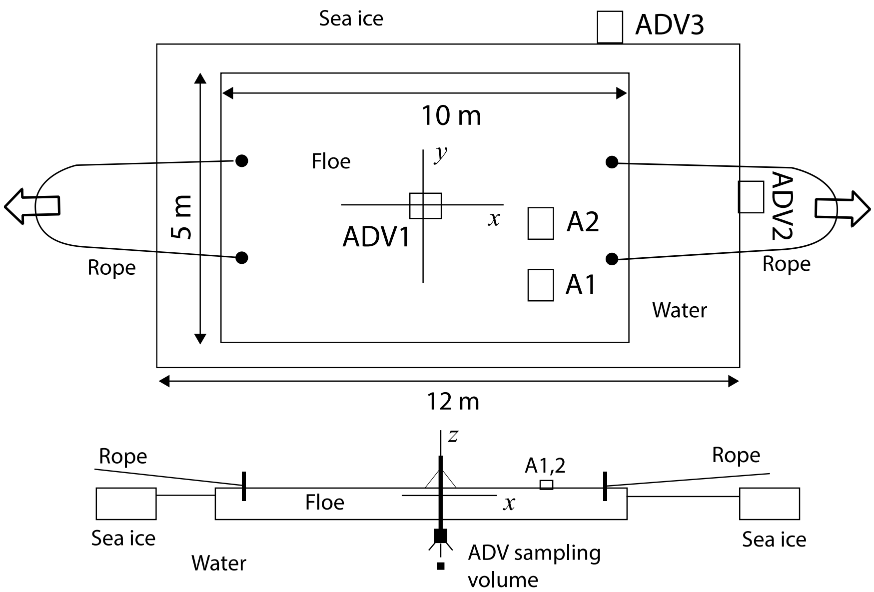

Figure 7. Sketch of the drift floe experiment. A1,2 are locations of accelerometers, ADV1,2,3 are locations of ADV velocity measurements.

Figure 8 shows an example of acceleration record in the drift floe experiment during four collisional interactions between the floe and the ice edges. The interaction events are marked 1,2,3,4 (Fig. 8a). The duration of each event is estimated at 1 s. Each event started from the floe deceleration during approaching to the ice edge, and consequent acceleration. The deceleration periods were shorter than the acceleration periods (Fig. 8 b,c). Integrals of the accelerations taken from $t = 0$ to t are shown in Fig. 8d versus time t. One can see that all integrals are practically equal to zero at $t = 3$ s. It means that floe-ice interaction follows the line 1 in Fig. 2b with $v_1 \approx v_0$. It can be explained by the floe rotation during the interaction events.

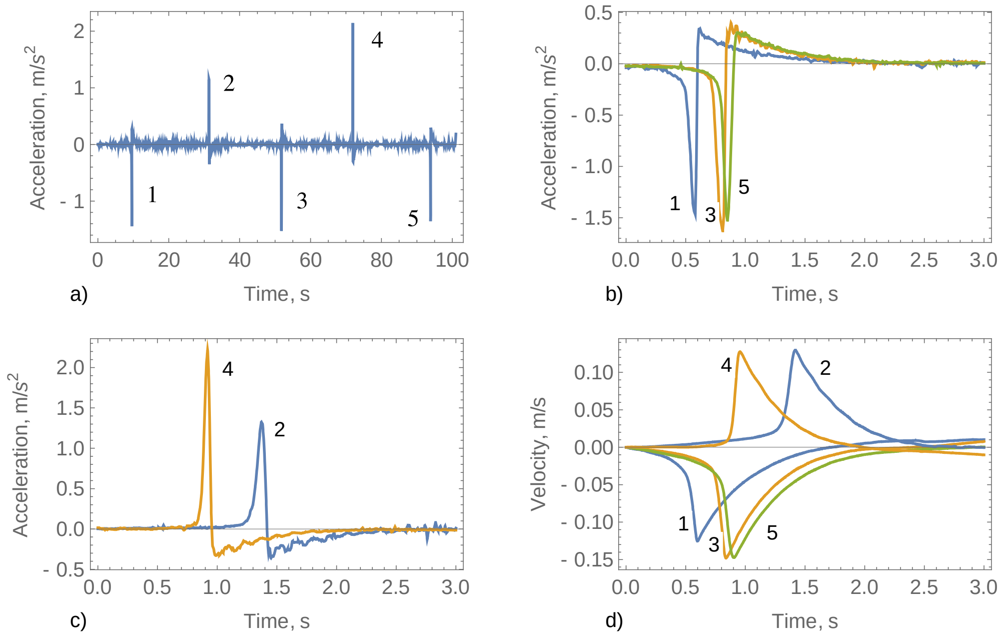

Figure 8. Example of acceleration record in the drift floe experiment. Accelerations recorded versus time after 4 collisions (a). Zoomed dependencies of the accelerations versus time (b,c), and integrated accelerations versus time (d).

Figure 9 shows an example of water velocities recorded by ADV during the experiment. Figures 9 a,b show the water velocities relative to the floe measured at a distance of 35 cm from the bottom surface of the floe (Location ADV1 in Fig. 7). Figure 10a shows zoomed fragment of this record together with the floe accelerations. The maximal absolute values of the velocities reached a few seconds after the collisions. The amplitudes of the horizontal velocities varied in the range between 20 cm/s and 30 cm/s, and the maximal amplitudes exceeded 30 cm/s. Figure 10 b shows the vertical water velocity below the floe versus time. The floe starts to move at $t = 880$ s, and the amplitude of the vertical velocity reaches a stable value already at $t = 1000$ s. Spectral density of the vertical velocity shown in Fig. 10 b demonstrated a good correlation with 5/3 slope corresponding to the Kolmogorov-Obukhov law for the developed turbulence (Kolmogorov, 1941; Obukhov,1941).

Figures 9 c,d show the horizontal and vertical water velocities recorded at the Location ADV2 at 50 cm from the bottom surface of the ice (Fig. 8). The maximal horizontal velocities reached 1 m/s, and the maximal vertical velocities exceeded 20 cm/s during the collisional interaction of the floe with the ice edges. One can see that each collision was accompanied by consequent events of downward (negative vertical velocity), upward (positive vertical velocity), and again downward motions of the water. Duration of each event was approximately 2 s. The water jets were seen on the ice surface during the collisions.

Figures 9 e,f show the horizontal and vertical water velocities recorded at the Location ADV3 at 65 cm from the bottom surface of the ice (Fig. 8). In this location the amplitude of the horizontal and vertical velocities of the water were of the same order of 5 cm/s. This measurement shows the velocity of water motion in the shear zone between the floe and the ice edges extended along the direction of the floe motion.

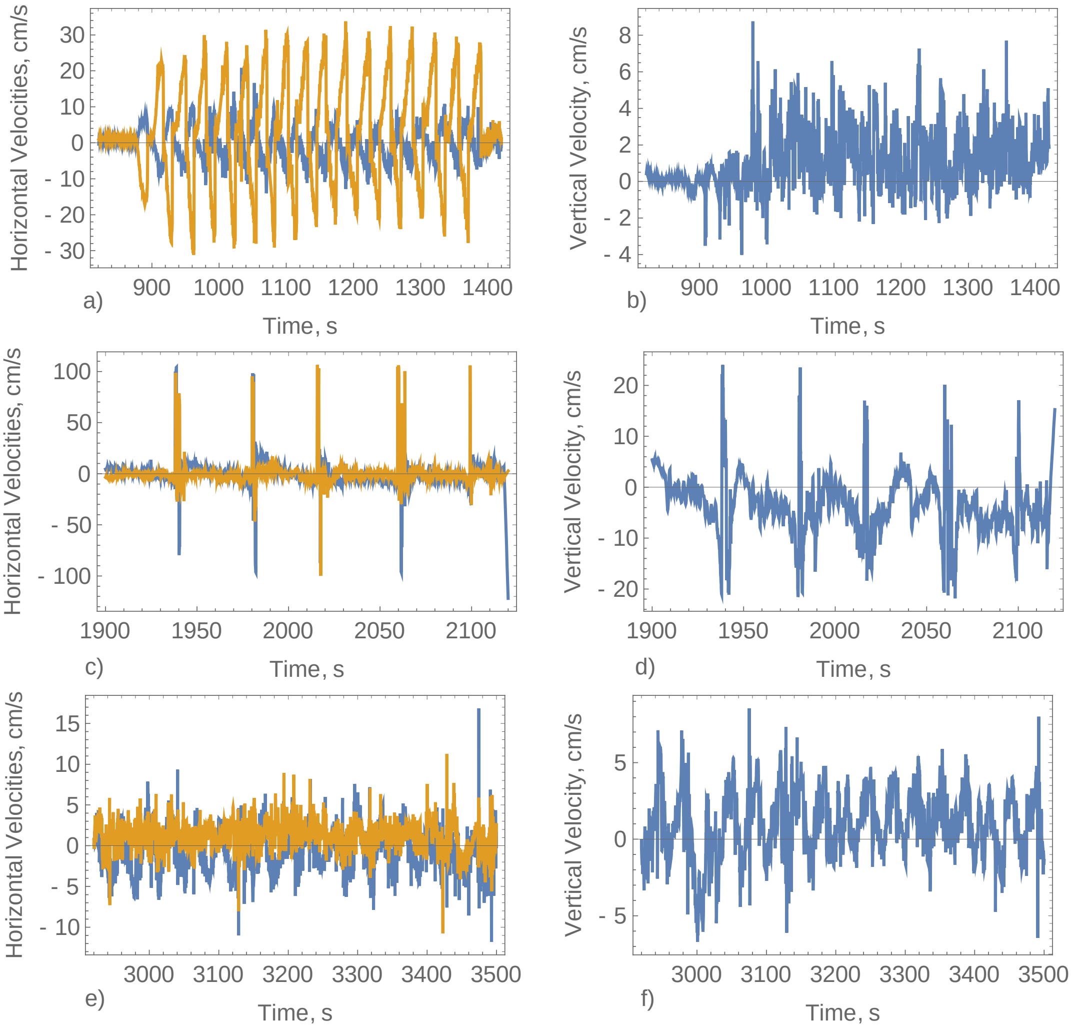

Figure 9. Example of the horizontal (a,c,d) and vertical (b,d,f) water velocities recorded by ADV versus time. The blue and yellow lines show respectively East and North velocities.

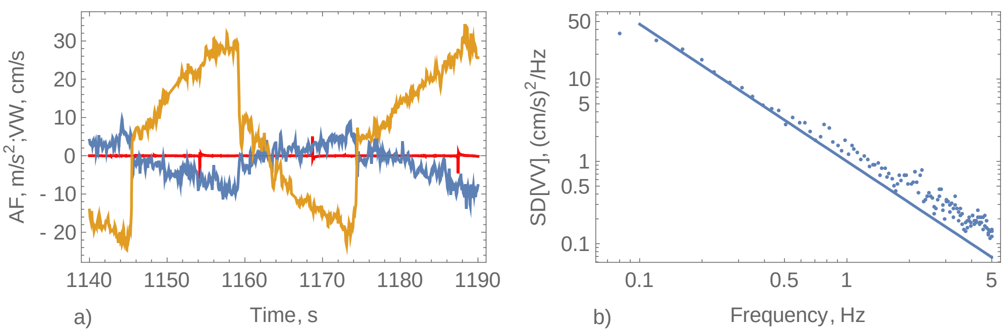

Figure 10. ADV1 measurements. Floe acceleration (AF, red line) and East (blue line) and North (yellow line) water velocities (VW) relative to the floe (VW) versus time (a). Spectral density of the vertical velocity (dotted line) and 5/3 slope (solid line).

The mean kinetic energy (KE) and kinetic energy of fluctuations (KEF) of the water motion are calculated from the formulas

$$2KE = \langle u^2 + v^2 + w^2 \rangle, \;\; 2KEF = \langle \delta u^2 + \delta v^2 + \delta w^2 \rangle, \tag{2}$$

where $\langle \ \rangle$ means averaging over the measurement time, u, v, and w are the velocities measured by ADV, and δu, δv, and δw are the velocity fluctuations. The calculated velocity fluctuations are equal to the differences between the actual and averaged velocities. The averaged velocities were calculated using the operation MovingAverage over 1 s applied to the actual data.

There are two time scales in the experiment. One time scale (~10 s) equals to the time interval of the floe motion between two consequent collisions. The other time scale equals to the ADV sampling interval set to 0.1 s. Averaging over 1 s extract "laminar" velocities initiated by the floe motion. The fluctuation velocities are related to the turbulent motion at smaller spatial scales initiated by the "laminar" velocities.

Table 1 shows the mean kinetic energy (KE) and the kinetic energy of fluctuations (KEF) of the water motion calculated from the measurements at locations ADV1, ADV2, and ADV3. KE is largest at the location ADV1, while KEF/KE is largest at the location ADV2. The minimal value of KE is reached at the location ADV3, while KEF/KE reaches the minimum at the location ADV1. This energy distribution is explained by the regular water motion below the central part of the floe, not regular water motion with strong fluctuations near the frontal edges of the floe colliding with the ice edges, and less intense, but still regular motion of the water near lateral edges of the floe.

Table 1. The mean kinetic energy (KE) and kinetic energy of fluctuations (KEF) of the water motion calculated from the ADV measurements.

	ADV1	ADV2	ADV3
KE·10^{-2}, $(cm/s)^2$	1.1	0.63	0.065
KEF·10^{-2}, $(cm/s)^2$	0.025	0.68	0.01
KEF/KE, %	2.2	100	17.1

DISCUSSION AND CONCLUSIONS

Two field experiments were performed to investigate ice-ice collisions and water motion initiated by the floe motion and collisions. We didn't observe significant ice breaking of the contacting surfaces of ice during each test, although gradual accumulation of slush in the water and some adjustment of the shapes of the contacting surfaces were seen after several tests in each experiment. We found that water pressure and floe rotation are important components of the collisional interaction. The action of water pressure increases the interaction time up to 1-2 s in comparison to the interaction time of about 0.01 s measured in the dry collision tests (Marchenko et al., 2019). The floes rotation influences the floe acceleration after the deceleration caused by the first contact and increases the interaction time in addition to the action of water pressure.

Cyclic motion of the floe influences currents and turbulence in the water. We observed the formation of developed turbulent motion of the water by cyclic motion of the floe (5m x10m) with a period of 20 s in a pool (5.5m x 12m) during 120 s. The integration of the floe acceleration over the time (Fig. 8d) showed that the floe velocity amplitudes were similar the water velocity amplitudes measured at 35 cm distance from the bottom surface of the floe (Fig. 9a). It means that the mean kinetic energy of the floe was of the order of the mean kinetic energy of the water. Therefore, relative motion of floes should have strong damping caused by the generation of turbulence in the upper ocean layer.

The dependence of floe acceleration on time shown in Fig. 8 is similar the dependence of floe accelerations on time obtained in the field experiment of (Martin and Becker, 1987; Fig. 4). In both cases floe accelerations were recorded immediately after the decelerations. It confirms the rotation of interacting floes caused by wave propagation below the ice. The acceleration amplitudes measured by Martin and Becker (1987) were below 5 mm/s2, that is 200-400 times smaller than in our tests. Therefore, energy dissipation during floe-floe collisions in the experiment of Martin and Becker (1987) was very small and indistinguishable in comparison with the energy of drift ice and water current below the ice.

ACKNOWLEDGEMENTS

The work was supported by the Research Council of Norway through the Petromks-2 project Dynamics of Floating Ice and IntPart project Arctic Offshore and Coastal Engineering in Changing Climate.

REFERENCES

Davis, R.H., Serayssol, J-M., Hinch, E.J., 1986. The elastohydrodynamic collision of two spheres. *J. Fluid Mech*., 163, 479-497.

De Carolis, G., Olla, P., Pignagnoli, L., 2005. Effective viscosity of grease ice in linearized gravity waves. *J. Fluid Mech*., 535, 369-381.

Joseph, G.G., Zenit, R., Hunt, M.L., Rosenwinkel, A.M., 2001. Particle-wall collisions in a viscous fluid. *J. Fluid Mech*., 433, 329-346.

Kolmogorov, A.N., 1941. The local structure of turbulence in incompressible vis-cous fluid for very large Reynolds number. *Dokl. Akad. Nauk SSSR*, 30:9–13.

Lamb, H.,1975. Hydrodynamics. Sixth Edition. Cambridge University Press.

Hongtao, Li., Lubbad, R., 2018. Laboratory study of ice floes collisions under wave action. *Proc. 28th Int. Ocean and Polar Eng. Conf.*, Sapporo, Japan, 1516-1524.

Marchenko, A., Markov, V., Taylor, R., 2019. Influence of Water on Collisions of Floating Ice Blocks. ISOPE, 19TPC-0906, 757-764.

Martin, S., Becker, P., 1987. High-frequency ice floe collisions in the Greenland Sea during the 1984 Marginal Ice Zone Experiment. *J. Geoph. Res*., 92, NC7, 7071-7084.

Morozov E.G., Marchenko A.V., Filchuk K.V., Kowalik Z., Marchenko N.A., and Ryzhov I.V. Sea ice evolution and internal wave generation due to a tidal jet in a frozen sea, *Applied Ocean Research*, 2019, Vol 87, P. 179-191

Obukhov, A.M., 1941. On the distribution of energy in the spectrum of turbulent flow. *Dokl. Akad. Nauk SSSR*, 32:19.

Starovoitov, V.N., 2003. Behavior of rigid body in an incompressible viscous fluid near a boundary. *Int. Series of Numerical Mathematics*, 147, 313-327.

Tchieu, A.A., Crowdy, D., Leonard, A., 2010. Fluid-structure interaction of two bodies in an inviscid fluid. *Physics of Fluid*, 22, 107101.